

Physics

Physics fields

Okayama University

Year 2004

Anisotropic diamagnetic response in
type-II superconductors with gap and
fermi-surface anisotropies

H Adachi
Okayama University

P Miranovic
University of Montenegro

M Ichioka
Okayama University

K Machida
Okayama University

This paper is posted at eScholarship@OUDIR : Okayama University Digital Information Repository.

http://escholarship.lib.okayama-u.ac.jp/physics_general/8

Anisotropic Diamagnetic Response in Type-II Superconductors with Gap and Fermi-Surface Anisotropies

H. Adachi,^{1,*} P. Miranović,² M. Ichioka,¹ and K. Machida¹

¹*Department of Physics, Okayama University, Okayama 700-8530, Japan*

²*Department of Physics, University of Montenegro, Podgorica 81000, Serbia and Montenegro*

(Received 15 October 2004; published 18 February 2005)

The effects of anisotropic gap structures on a diamagnetic response are investigated in order to demonstrate that the field-angle-resolved magnetization [$M_L(\chi)$] measurement can be used as a spectroscopic method to detect gap structures. Our microscopic calculation based on the quasiclassical Eilenberger formalism reveals that $M_L(\chi)$ in a superconductor with a fourfold gap displays a fourfold oscillation reflecting the gap and Fermi-surface anisotropies, and the sign of this oscillation changes at a field between H_{c1} and H_{c2} . As a prototype of unconventional superconductors, magnetization data for borocarbides are also discussed.

DOI: 10.1103/PhysRevLett.94.067007

PACS numbers: 74.25.Op, 74.25.Ha, 74.70.Dd

A precise determination of the node position or gap structure is of fundamental importance in superconductivity study in general, especially for ever-growing so-called unconventional superconductors, since it is indispensable in identifying the pairing mechanism for a material of interest. There are only a few established methods for the precise determination of gap structures; angle-resolved specific heat and thermal conductivity measurements are notable ones [1–5]. Nevertheless, to reinforce the conclusion, more such spectroscopic experiments based on bulk quantities are desirable [6]. As Takanaka [7] suggested within the Ginzburg-Landau (GL) theory, a diamagnetic response is a strong candidate if combined with an analysis of the basal plane magnetization anisotropies. Needless to say, a diamagnetic response from a superconductor is a hallmark of rigidity of the macroscopic wave function, containing a wealth of microscopic information, and it is a routine work to measure magnetizations to check if a material of interest is a superconductor or not. Since we are realizing [5] that field-angle dependences of various physical quantities such as specific heat or thermal conductivity should reflect low-lying quasiparticles around the vortex core, it is also expected that the magnetization contains the same kind of information.

Among a vast amount of type-II superconductors, nonmagnetic borocarbides RNi_2B_2C ($R = Lu, Y$) are considered to be typical examples of unconventional ones in the following sense: (i) Lots of experiments have demonstrated the existence of gap nodes (or gap minima) [1,2,8–10]; (ii) the normal and mixed states are not exposed to the strong fluctuations such as in cuprates; (iii) there exist detailed magnetization measurements [11,12]. To establish a spectroscopic method based on the magnetization measurements, it is thus important to understand the anisotropic diamagnetic response in these materials and clarify its relation to the gap structure.

In the works by Civale *et al.* [11] and Kogan *et al.* [12], basal plane magnetizations were measured as a function of

the angle χ (see Fig. 1) between the applied field and the crystal axis, and it was found that the fourfold oscillation of the magnetization showed a sign reversal with decreasing the field (or temperature). Kogan *et al.* [12] demonstrated that these behaviors can be reproduced within a nonlocal London theory without quoting anisotropy effects of the gap function. However, at least when discussing anisotropy effects in a vortex state, the validity of the London description in high fields is quite unclear since the framework is appropriate only in a field region $H \ll H_{c2}$. If we aim to clarify whether the observed phenomena are generic ones or not, we need a theoretical approach which can correctly describe the anisotropy of H_{c2} and the core effects.

The purpose of this Letter is twofold. The first one is to clarify the effects of gap structures on the anisotropic diamagnetic response based on the quasiclassical Eilenberger formalism. The second one is to apply our analysis to the prototype materials, i.e., nonmagnetic borocarbides, and present a microscopic description of the observed mysterious sign reversal of the $M_L(\chi)$ oscillation [11,12]. Our microscopic treatment covers, of course, both

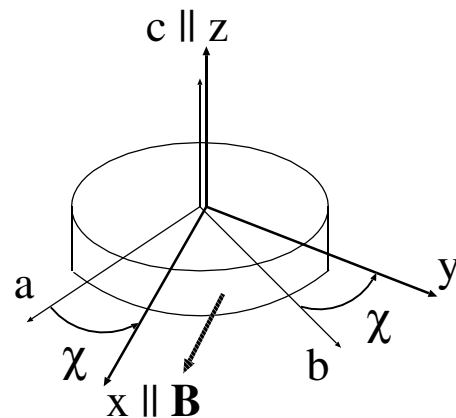


FIG. 1. The coordinates (x, y, z) and the crystal axes (a, b, c) . The induction \mathbf{B} is rotated from the a axis by an angle χ .

GL theory and London theory, since the former is derived from the Eilenberger formalism through an expansion about the pair field, while the latter is derived by using a phase only (London) approximation. Indeed, our numerical solution at finite temperatures well reproduces both GL behavior ($M \propto H_{c2} - B$) near H_{c2} and London behavior [$M \propto \ln(H_{c2}/B)$] in lower fields.

Let us first explain our numerical procedure. We start with the following Eilenberger equation [13] ($k_B = \hbar = 1$):

$$f(\varepsilon_n, \mathbf{p}, \mathbf{r}) = (2\varepsilon_n + i\mathbf{v} \cdot \mathbf{\Pi})^{-1} (2g(\varepsilon_n, \mathbf{p}, \mathbf{r})w_{\mathbf{p}}\Delta(\mathbf{r})), \quad (1)$$

where $f(\varepsilon_n, \mathbf{p}, \mathbf{r})$, $f^\dagger(\varepsilon_n, \mathbf{p}, \mathbf{r}) = f^*(\varepsilon_n, -\mathbf{p}, \mathbf{r})$ and $g(\varepsilon_n, \mathbf{p}, \mathbf{r}) = \sqrt{1 - f(\varepsilon_n, \mathbf{p}, \mathbf{r})f^\dagger(\varepsilon_n, \mathbf{p}, \mathbf{r})}$ are the Eilenberger's Green's functions. Here $\varepsilon_n = 2\pi T(n + 1/2)$ is a fermionic Matsubara frequency, \mathbf{v} is a Fermi velocity, $\mathbf{\Pi} = -i\nabla + (2\pi/\Phi_0)\mathbf{A}$ is a gauge invariant gradient, T_c is a transition temperature at a zero field, and Φ_0 is the flux quantum. The gap function is expressed as $\Delta_{\mathbf{p}}(\mathbf{r}) = w_{\mathbf{p}}\Delta(\mathbf{r})$ where $w_{\mathbf{p}}$ is the pairing function with relative momentum \mathbf{p} of the Cooper pair, and $\Delta(\mathbf{r})$ is the order parameter with center of mass coordinate \mathbf{r} . Throughout this Letter we treat extreme type-II superconductors with large GL parameter $\kappa \gg 1$ (in borocarbide superconductors $\kappa \gtrsim 10$), so that the vector potential is approximated by $\mathbf{A} = -Bz\hat{\mathbf{y}}$ where $\mathbf{B} = B\hat{\mathbf{x}}$ is the induction (see Fig. 1). This is indeed a good approximation in the high- κ case since the correction term is of order $O(1/\kappa^2)$. To solve Eq. (1), we adopt an approximation similar to that used by Pesch [14],

$$f \approx 2gw_{\mathbf{p}}(2\varepsilon_n + i\mathbf{v} \cdot \mathbf{\Pi})^{-1}\Delta. \quad (2)$$

The physics behind this approximation is that the spatial variation of f related to the phase modulation of Δ is much larger than the spatial variation of g describing the amplitude fluctuation. It is worth noting that we do not replace g in the above equation by its spatial average, as Pesch has done, in order to ensure that the correct expressions for the nonlocal GL free energy F/V given in Ref. [15] are reproduced up to the quartic term. Besides the above mentioned justification near H_{c2} , the applicability to lower fields is improved by requiring the self-consistency among f , f^\dagger , and g . Furthermore, our scheme can be valid in an anisotropic case by including the contribution of higher Landau level components to Δ :

$$\Delta = \Delta_0 \sum_{N=0}^{N_{\max}} d_N \psi_N, \quad (3)$$

$$\psi_N = \sum_{m=-\infty}^{\infty} C_m \frac{H_N(z + \nu m)}{\sqrt{2^N N!}} e^{-(z + \nu m)^2/2 - i\nu m y}, \quad (4)$$

where $\Delta_0 = 1.764T_c$, $r_B = \sqrt{\phi_0/2\pi B}$, $C_m = (\nu r_B/\sqrt{\pi})e^{-i\pi\zeta m^2}$, H_N is the N th Hermite polynomial,

and the lengths are measured in units of r_B . The real constants ζ and ν specify the configuration of a vortex lattice. Since the difference of a vortex lattice configuration is considered to be irrelevant to the quantity in question, we set in this Letter $\zeta = 1/2$ and $\nu = \sqrt{\sqrt{3}\pi}$, the value for a triangular lattice. Substituting the above expression into Eq. (2) and using a parameter representation ($2\varepsilon_n + i\mathbf{v} \cdot \mathbf{\Pi})^{-1} = \int_0^\infty d\rho e^{-(2\varepsilon_n + i\mathbf{v} \cdot \mathbf{\Pi})\rho}$, we have

$$f = 2gw_{\mathbf{p}} \int_0^\infty d\rho e^{-2\varepsilon_n \rho} \left(\Delta_0 \sum_{N=0}^{N_{\max}} \alpha_N d_N \right). \quad (5)$$

Here the expression for $\alpha_N \equiv e^{-i\rho\nu \cdot \mathbf{\Pi}} \psi_N$ is given by

$$\alpha_N = \sum_m C_m \frac{H_N(z + \nu m - \text{Re } \lambda)}{\sqrt{2^N N!}} \times e^{-(|\lambda|^2 - \lambda^2)/4} e^{-(z + \nu m - \lambda)^2/2 - i\nu m y}, \quad (6)$$

where $\lambda = (v_z + iv_y)\rho/r_B$. At long last we have a solution for f , on condition that we have the correct $\{d_N\}$ values. To determine $\{d_N\}$ we use the following self-consistent equation projected onto each Landau level:

$$\left[\ln\left(\frac{T}{T_c}\right) + 2\pi T \sum_{n \neq 0} \varepsilon_n^{-1} \right] d_N = \frac{2\pi T}{\Delta_0} \sum_{n \neq 0} \overline{\psi_N^* \langle w_{\mathbf{p}}^* f \rangle}, \quad (7)$$

where the overbar denotes the spatial average, and the Fermi surface (FS) average $\langle \dots \rangle$ satisfies a normalization condition $\langle 1 \rangle = 1$; the definition is given by Eq. (9) below. Our numerical procedure is as follows: Input initial values for $\{d_N\}$, f , f^\dagger , and g . Next use Eq. (5) to obtain the new f (and f^\dagger , g). Then iterate Eq. (7) to renew the $\{d_N\}$ values, and return to Eq. (5). In order to check the reliability of our numerical procedure, we initially treated a two-dimensional case and calculated field dependences of each $\{d_N\}$ at $T/T_c = 0.5$. The obtained result was quite similar to the previous work based on the Landau level expansion of the GL equation [Figure 2(b) of Ref. [16]]. In the following calculation we use $N_{\max} = 6$.

The magnetization $4\pi\mathbf{M} = \mathbf{B} - \mathbf{H}$ is obtained from the relation $\mathbf{H} = 4\pi\nabla_{\mathbf{B}}(F/V)$. As for the longitudinal component $\mathbf{M}_L(\parallel \mathbf{H})$, which we focus on in this Letter, Klein *et al.* [17] obtained a more convenient formula extending the virial theorem derived by Doria *et al.* [18]:

$$-4\pi M_L = \frac{2\pi^2 N(0)}{B} T \sum_{n \neq 0} \left\langle \frac{\sqrt{2g[f^\dagger(w_{\mathbf{p}}\Delta) + f(w_{\mathbf{p}}\Delta)^*]}}{1 + g} - 4\varepsilon_n(1 - g) \right\rangle, \quad (8)$$

where in the above equation we approximately set $\mathbf{B} \cdot \mathbf{H} \simeq BH$ as in Ref. [12].

Now let us assume an isotropic FS to focus only on the role of the gap anisotropy. In this case the Fermi momentum can be written as $\mathbf{p} = mv_0\hat{r}$, where $\hat{r} = (\sin\theta \cos\phi, \sin\theta \sin\phi, \cos\theta)$, v_0 is the Fermi velocity in

the isotropic case, and m is the effective mass of the quasiparticle. As a model for an anisotropic gap function, $w_{\mathbf{p}} = \sqrt{1 - \alpha \cos 4(\phi + \chi)} / \langle 1 - \alpha \cos 4(\phi + \chi) \rangle$ is used where χ is the field angle measured from the crystal a axis, and ϕ is the azimuthal angle measured from the x axis. Thus α denotes the degree of the gap anisotropy with $\alpha = 1$ being the nodal case. Figure 2 shows the field dependence of the longitudinal magnetization M_L for $\mathbf{B} \parallel$ node (filled circles) and $\mathbf{B} \parallel$ antinode (open circles) at $T = 0.6T_c$. From the inset both the GL and the London behaviors are clearly seen. Although the difference of M_L between the two field orientations is rather small, we can find that the M_L at $B \approx H_{c2}$ is larger for the $\mathbf{B} \parallel$ node, but with lowering the field this tendency is reversed at a field B^* . In Fig. 3(a), the corresponding field-angle dependences of $M_L(\chi)$ are plotted for several inductions. It should be emphasized here that the gap anisotropy *alone* can cause a sign reversal of the $M_L(\chi)$ oscillation. The result with isotropic FS can be summarized as follows: $M_L^{B \parallel \text{node}} > M_L^{B \parallel \text{antinode}}$ in higher fields, and $M_L^{B \parallel \text{antinode}} > M_L^{B \parallel \text{node}}$ in lower fields.

Next we discuss the magnetization experiments [11,12] for borocarbides. The observed data are incompatible with the above conclusion once we recall the experimental suggestion that the nodes exist along the [100] and [010] directions [1,2]. The discrepancy is considered to stem from the *unusually* large FS anisotropy possessing partial nesting [19] in these materials. As a model having such an anisotropic FS, we introduce a fourfold anisotropic dispersion $\epsilon_{\mathbf{p}} = \frac{1}{2m} \{ (p_x^2 + p_y^2)[1 + \beta \cos 4(\phi + \chi)] + p_z^2 \} = \frac{v^2}{2m} \sigma^2$ where $\sigma(\theta, \phi) = \sqrt{1 + \beta \sin^2 \theta \cos 4(\phi + \chi)}$. Thus β denotes the degree of the FS anisotropy. The resultant Fermi momentum can be written as $\mathbf{p} = (mv_0/\sigma)\hat{r}$. The Fermi

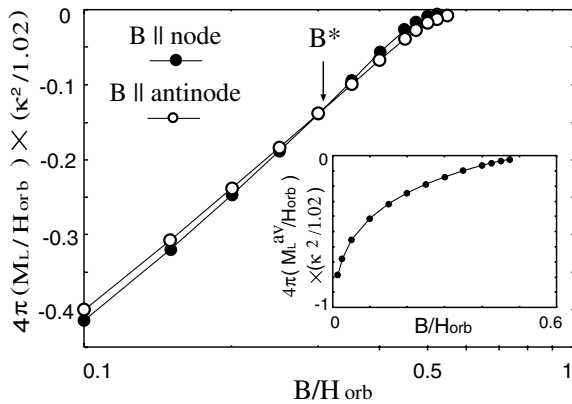


FIG. 2. Logarithmic field dependence of longitudinal magnetization M_L at $T/T_c = 0.6$ for $\mathbf{B} \parallel$ node (filled circles) and $\mathbf{B} \parallel$ antinode (open circles). The used anisotropy parameters are $\alpha = 1$ and $\beta = 0$. $H_{\text{orb}} = 1.037\Phi_0/2\pi\xi_0^2$ ($\xi_0 = v_0/2\pi T_c$) is the orbital limiting field in the isotropic case. Inset: Field dependence of $M_L^{\text{av}} = [M_L(\chi = 0) + M_L(\chi = \pi/4)]/2$ for the same parameters.

velocity $\mathbf{v} = \nabla_{\mathbf{p}}\epsilon_{\mathbf{p}}$ can be expressed as $\mathbf{v} = v_r\hat{r} + v_\theta\hat{\theta} + v_\phi\hat{\phi}$, where $\hat{\theta} = (\cos\theta\cos\phi, \cos\theta\sin\phi, -\cos\theta)$ and $\hat{\phi} = (-\sin\phi, \cos\phi, 0)$. Here each component of \mathbf{v} is given by $v_r = v_0\sigma$, $v_\theta = 2v_0(\beta/\sigma)\sin^3\theta\cos\theta\cos 4(\phi + \chi)$, and $v_\phi = -2v_0(\beta/\sigma)\sin^3\theta\sin 4(\phi + \chi)$. Finally, the area element dS of the FS divided by $|\mathbf{v}|$ is given by $dS/|\mathbf{v}| = (m^2v_0/\sigma^3)d(\cos\theta)d\phi$. Then our definition of the FS average is given by

$$\langle A_{\mathbf{p}} \rangle = \frac{\int_{\text{FS}} (dSA_{\mathbf{p}}/|\mathbf{v}|)}{\int_{\text{FS}} (dS/|\mathbf{v}|)}. \quad (9)$$

A band structure calculation for $\text{LuNi}_2\text{B}_2\text{C}$ suggests a rough estimate $\beta \approx 0.4$ so as to reproduce the ratio $\langle v_a^4 \rangle / \langle v_a^2 v_b^2 \rangle = 0.128$ [20] within our model.

Starting from the isotropic FS case ($\beta = 0$) and increasing the β value, the oscillation pattern seen in Fig. 3(a) first tends to diminish, and, when the β value exceeds about 0.1, the sign of the $M_L(\chi)$ -oscillation pattern is completely reversed. This is shown in Fig. 3(b), and the oscillation behavior well coincides with the results of Refs. [11,12]. Worth noting is that $\alpha\beta > 0$ in our model corresponds to the *competing anisotropy* case in the sense of Ref. [21], where the observed configuration [22] of the vortex lattice in $\mathbf{B} \parallel c$ is properly explained by the competition between gap and FS anisotropies. Note also that the main conclusion here is not changed by the nodal topology and effective dimensionality of a material, though the oscillation amplitude is *quantitatively* enhanced for a quasi-two-dimensional material.

We show in Fig. 4 the field dependence of the magnetization oscillation amplitude $\delta M_L = M_L(\chi = \pi/4) - M_L(\chi = 0)$ at $T/T_c = 0.6$, which is to be compared with the experiments (Fig. 3 of Ref. [11] and Fig. 5 of Ref. [23]). The characteristic behavior that δM_L is a slowly increasing function of the field except for a peak

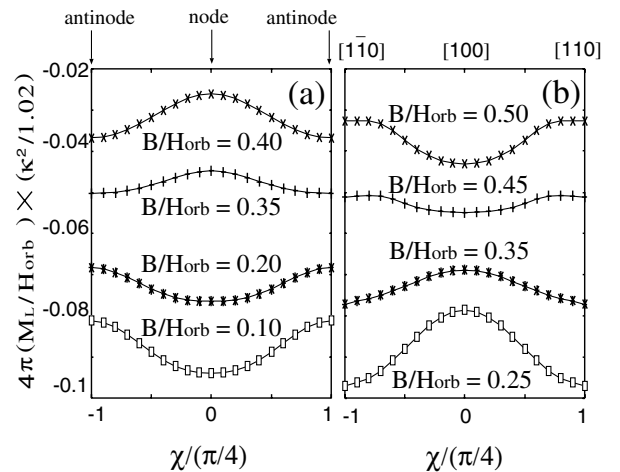


FIG. 3. Field-angle dependences of $M_L(\chi)$ for (a) $\alpha = 1, \beta = 0$ and (b) $\alpha = 1, \beta = 0.4$ at $T/T_c = 0.6$ for several inductions. The data at different B are vertically shifted.

structure slightly below H_{c2} is well reproduced. Finally, the inset of Fig. 4 shows the oscillation sign reversal field B^* in the B - T phase diagram for $\alpha = 1$ and $\beta = 0.4$. The $B^*(T)$ is a decreasing function of the temperature, and this is consistent with the experimental finding of Ref. [24]. The $B^*(T)$ could be a diagnostic quantity to characterize the gap function and the FS anisotropy.

The physics behind the phenomena is explained as follows: Near H_{c2} where the GL theory can be applied, the anisotropy of the longitudinal magnetization $4\pi M_L \approx (B - H_{c2})/2.32\kappa^2$ comes from that of H_{c2} . In lower fields where the London theory is more appropriate, the anisotropy of $4\pi M_L \approx (-\Phi_0/8\pi\lambda^2) \ln(H_{c2}/B)$ is effectively attributed to that of the penetration depth λ . Extending knowledge of the relation between the ξ and the λ anisotropies based on the anisotropic GL equation [25], a naive relation $H_{c2}(\chi = 0)/H_{c2}(\chi = \pi/4) \sim \lambda^2(\chi = 0)/\lambda^2(\chi = \pi/4)$ is expected to hold, where $\lambda(\chi)$ means an effective penetration depth perpendicular to $H_{c2}(\chi)$. Namely, if H_{c2} is larger, then $1/\lambda^2$ is expected to be smaller, and this causes the sign reversal of the $M_L(\chi)$ oscillation.

Before ending we briefly discuss the origin of the peculiar angular variation of $M_L(\chi)$ seen in Refs. [11,12]. The low field $M_L(\chi)$ [11,12] have sharp maxima around the [100] and [010] directions, and broader minima around the [110] and $[\bar{1}\bar{1}0]$ directions. The sharp maxima remind us of the observed cusplike minima of thermal conductivity and specific heat [1,2] around the [100] and [010] directions. These have been argued as a result of the so-called “ $s + g$ ” pairing function [1]. We calculated $M_L(\chi)$ for the pairing $w_{\mathbf{p}} \propto [1 - \sin^4\theta \cos 4(\phi + \chi)]$ with point nodes keeping $\beta = 0.4$. However, no such characteristic structure was observed in the angular dependence of $M_L(\chi)$. This means that explanations for the observed structure of $M_L(\chi)$ may need a different mechanism.

In conclusion, we have microscopically studied field-angle-resolved basal plane magnetization oscillations, and demonstrated not only that a careful measurement of the magnetization can be a potentially useful tool to identify the nodal position of the gap function when a material of interest possesses less anisotropic FS, but also that the experimental data for borocarbides are well reproduced by considering both gap and FS anisotropies. If combined with other field-angle-resolved quantities [26], such as specific heat and thermal conductivity at low temperatures, we can further narrow the possible pairing symmetry or gap anisotropy in various conventional and unconventional superconductors. The lesson from borocarbides tells us that for materials with unusually strong FS anisotropy such as borocarbides we should be careful to judge the nodal position through magnetization measurements, since unusually strong FS anisotropy can reverse the conclusion.

After the submission of the first manuscript we learned about a preprint by Kusunose [27] which studies the effect

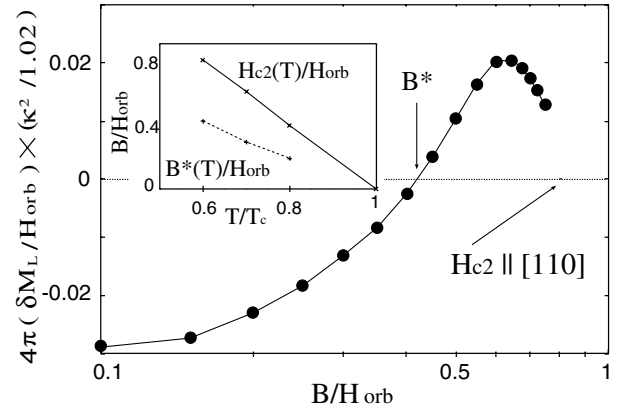


FIG. 4. Logarithmic field dependence of $\delta M_L = M_L(\chi = \pi/4) - M_L(\chi = 0)$ for $\alpha = 1, \beta = 0.4$ at $T/T_c = 0.6$. Inset: The sign reversal field B^* in the B - T phase diagram. The H_{c2} is determined through linear extrapolations of M_L .

of the gap anisotropy alone based on a simplified version of our treatment. The result is consistent with ours when only gap anisotropy is considered.

We acknowledge useful discussions with T. Sakakibara and Y. Matsuda.

*Electronic address: adachi@mp.okayama-u.ac.jp

- [1] K. Izawa *et al.*, Phys. Rev. Lett. **89**, 137006 (2002).
- [2] T. Park *et al.*, Phys. Rev. Lett. **90**, 177001 (2003); see also cond-mat/0411001.
- [3] K. Izawa *et al.*, Phys. Rev. Lett. **87**, 057002 (2001).
- [4] H. Aoki *et al.*, J. Phys. Condens. Matter **16**, L13 (2004).
- [5] P. Miranović *et al.*, Phys. Rev. B **68**, 052501 (2003).
- [6] There is an ongoing controversy on the gap function: either $d_{x^2-y^2}$ [3] or d_{xy} [4] pairings in CeCoIn₅.
- [7] K. Takanaka, J. Phys. Soc. Jpn. **65**, 3396 (1996).
- [8] M. Nohara *et al.*, J. Phys. Soc. Jpn. **68**, 1078 (1999).
- [9] T. Yokoya *et al.*, Phys. Rev. Lett. **85**, 4952 (2000).
- [10] I.-S. Yang *et al.*, Phys. Rev. B **62**, 1291 (2000).
- [11] L. Civale *et al.*, Phys. Rev. Lett. **83**, 3920 (1999).
- [12] V. G. Kogan *et al.*, Phys. Rev. B **60**, R12577 (1999).
- [13] G. Eilenberger, Z. Phys. **214**, 195 (1968); see also N. Schopohl, J. Low Temp. Phys. **41**, 409 (1980).
- [14] W. Pesch, Z. Phys. B **21**, 263 (1975).
- [15] H. Adachi and R. Ikeda, Phys. Rev. B **68**, 184510 (2003).
- [16] T. Kita, J. Phys. Soc. Jpn. **67**, 2067 (1998).
- [17] U. Klein and B. Pöttinger, Phys. Rev. B **44**, 7704 (1991).
- [18] M. M. Doria *et al.*, Phys. Rev. B **39**, 9573 (1989).
- [19] S. B. Dugdale *et al.*, Phys. Rev. Lett. **83**, 4824 (1999).
- [20] V. G. Kogan *et al.*, Phys. Rev. B **55**, R8693 (1997).
- [21] N. Nakai *et al.*, Phys. Rev. Lett. **89**, 237004 (2002).
- [22] M. R. Eskildsen *et al.*, Phys. Rev. Lett. **86**, 5148 (2001).
- [23] J. R. Thompson *et al.*, Phys. Rev. B **64**, 024510 (2001).
- [24] L. Civale *et al.*, Physica (Amsterdam) **341-348C**, 1299 (2000).
- [25] L. P. Gor'kov *et al.*, Sov. Phys. JETP **18**, 1031 (1964).
- [26] P. Miranović *et al.*, cond-mat/0409371.
- [27] H. Kusunose, cond-mat/0411540.